Dalton Transactions

PAPER

View Article Online
View Journal | View Issue

Cite this: *Dalton Trans.*, 2015, **44**, 17209

Bridged bis-BODIPYs: their synthesis, structures and properties†

Praseetha E. Kesavan,[a] Sudipta Das,[a] Mohsin Y. Lone,[b] Prakash C. Jha,[b] Shigeki Mori[c] and Iti Gupta*[a]

Received 22nd May 2015,
Accepted 25th August 2015

DOI: 10.1039/c5dt01925g

www.rsc.org/dalton

A series of bis-BODIPYs **1–6** bridged *via* thiophene, furan, *N*-alkylcarbazole, triphenyl-amine, *para*- and *meta*-phenylene groups have been synthesized and characterized by various spectroscopic techniques. The change in the spectroscopic properties of bis-BODIPYs upon varying the size of spacers was studied. X-ray crystal structures of three bis-BODIPYs containing triphenylamine, *para*- and *meta*-phenylene bridges were solved. Intermolecular C(H)···π and π···π stacking interactions were observed in solid state structures of three bis-BODIPYs. The dihedral angles between the spacer unit and two boron-dipyrrin units were lower in all three compounds as compared to their corresponding monomers. This suggests increased interactions between the two boron-dipyrrin units in molecules which are in turn reflected in the anodic shifts in their reduction potentials. DFT studies indicated effective electronic interactions between spacers and two boron dipyrrin units in all the bis-BODIPYs. The calculated HOMO–LUMO gap was found to be lower for bis-BODIPY having bulky carbazole spacers and higher for bis-BODIPY having smaller furan spacers. Changing the spacer size clearly affected the spectroscopic properties of the bis-BODIPYs and red shifted absorption and emission maxima were observed for bis-BODIPYs with furan and thiophene spacers as compared to bis-BODIPYs with phenylene or bulky aromatic spacers.

Introduction

Covalently linked pairs of chromophores have been a matter of interest for the scientific community for a long time. Such chromophore dimers have been found in biology, for example, photosynthetic bacterial proteins and natural light harvesting antenna systems.[1–3] Numerous artificial fluorescent dyes have been used in biosciences for cell imaging and investigation of *in vivo* biological processes. The boron dipyrromethenes (BODIPYs) are a well-known class of highly emissive molecules and they have been found to be extremely useful for biological applications, *e.g.* biochemical labelling,[4–6] photosensitizers for PDT (Photo Dynamic Therapy)[7] and fluorescent probes.[8–10]

The electronic and photophysical properties of BODIPYs can be fine-tuned for different applications by the structural modification of the boron-dipyrrin core or by making their dimers and oligomers.[11] Substitution at *meso* positions of the boron dipyrrin core with bulky electron rich heterocycles could produce large Stokes shifts of 100–120 nm.[12] β–β Linked dimers, *meso–meso* linked dimers and cofacial BODIPY dimers have been synthesised and studied.[13–15] Such artificial BODIPY dimers possess increased Stokes shifts, broad absorption and red shifted emission for efficient light harvesting ability for solar cell and biological applications. Recently Akkaya *et al.* have demonstrated that *meso–meso* and *meso-beta* linked BODIPY dimers can be used as singlet oxygen photosensitizers in nonpolar organic media.[16] Li and co-workers have synthesized β–β linked BODIPY dimers with triphenylsilylphenyl groups for increased solid state emission.[17] Bithiophene bridged BODIPY dimers have been prepared by Ziessel and co-workers with red shifted absorption and emission for future application as NIR fluorescent probes.[18] Interesting symmetry breaking ICT (intramolecular charge transfer) properties have been observed for *p*-phenylene bridged α-alkylated BODIPY dimers.[19] Nishihara and co-workers have reported *p*-diethynylphenyl bridged BODIPY dimers and *meso*-alkynyl BODIPY with red shifted emission maxima.[20] Liu *et al.* have synthesized triphenylamine BODIPY monomers, bridged dimers and trimers

[a]*Indian Institute of Technology Gandhinagar, VGEC Campus, Chandkheda, Ahmedabad-382424, India. E-mail: iti@iitgn.ac.in; Fax: +91-23972324; Tel: +91-9925479623*
[b]*School of Chemical Sciences, Central University of Gujarat, Gandhinagar 382030, Gujarat, India*
[c]*Integrated Centre for Sciences, Ehime University, Matsuyama 790-8577, Japan*

† Electronic supplementary information (ESI) available: The synthetic procedures of some starting materials, characterization data like HRMS, ^{1}H, ^{13}C, ^{19}F, and ^{11}B NMR spectra, fluorescence decay profiles, DFT calculation and X-ray structure details of reported compounds. CCDC 1006185, 1006186 and 1028232. For ESI and crystallographic data in CIF or other electronic format see DOI: 10.1039/c5dt01925g

in a one pot reaction and their lasing properties in organic media were studied.[21] BODIPY dimers having bipyridine spacers with interesting ECL (electrogenerated chemiluminescence) properties have been reported by Bard and co-workers.[22] Benniston and co-workers have synthesized cofacial BODIPY dimers containing dibenzothiophene and dibenzofuran moieties; such dimers formed intramolecular excimers in emission studies.[23] Saki *et al.* have designed cofacial BODIPY dimers based on the xanthene scaffold with efficient energy transfer between the two boron dipyrrin units.[24] Reports on covalently linked BODIPY dimers are on the rise but still there is a need to study the photophysical properties of *meso*-phenylene and heterocycle bridged BODIPY dimers. In this article we present the synthesis, crystal structures, photophysical and electrochemical properties of thiophene, furan, *N*-butyl carbazole, triphenylamine, *p*- and *m*-phenylene bridged bis-BODIPYs. Also, DFT studies were carried out for all six bis-BODIPYs and the HOMO–LUMO energy gap was calculated.

Results and discussion

The stepwise synthesis of bis-BODIPYs **1–6** is depicted in Schemes 1–3. The corresponding key precursors such as bis-aromatic aldehydes were prepared by a Vilsmeier–Haack formylation reaction and bis-dipyrranes **7–12** were synthesized as per a reported procedure.[25] Terephthalaldehyde and isophthalaldehyde were condensed with pyrrole in the presence of a catalytic amount of indium chloride to form bis-dipyrranes **7** and **8** respectively (Scheme 1). Crude dipyrranes **7** and **8** were purified by silica gel column chromatography using a 1 : 2 : 4 mixture of ethyl acetate/dichloromethane/petroleum ether in 29% and 46% yields respectively. The corresponding bis-aldehydes for bis-dipyrranes **9** and **10** were prepared by a Vilsmeier–Haack formylation reaction as per a reported procedure[25] (ESI†). Bis-dipyrranes **9** and **10** were synthesized by the indium chloride method[25] followed by silica gel column purification in 55% and 41% yields respectively (Scheme 2). The bis-dipyrranes **7–10** were oxidized by 2.4 equivalents of DDQ (2,3-dichloro-5,6-dicyano-1,4-benzoquinone) and the resulting bis-dipyrrins were then complexed with $BF_3{\cdot}OEt_2$ by doubling the equivalents of reagents required for the standard BODIPY synthesis.[26]

Silica gel column chromatographic purification afforded bis-BODIPYs **1–4** as solid powders in 8–33% yields (Schemes 1 and 2). In order to synthesize bis-BODIPYs **5** and **6**, bis-formyl derivatives of thiophene and furan were prepared (Scheme 3) by dilithiation of thiophene and furan followed by the addition of dry DMF (*N*,*N*-dimethylformaldehyde). The bis-formylthiophene and furan were subjected to acid catalysed condensation with pyrrole to obtain the corresponding bis-dipyrranes **11** and **12**. The crude bis-dipyrranes **11** and **12** were directly used further for the next step without any purification due to their instability under column conditions. The bis-dipyrranes **11** and **12** were reacted with DDQ followed by complexation with $BF_3{\cdot}OEt_2$ in the presence of TEA (triethylamine, Scheme 3). Silica gel column chromatographic purification of the crude reaction mixture in a 60–70% dichloromethane/petroleum ether mixture yielded 8% of bis-BODIPY **5** as a dark orange solid and 10% of bis-BODIPY **6** as a dark brown solid.

Bis-dipyrranes **7–10** were characterized by HRMS and ^{1}H NMR spectroscopy. Bis-BODIPYs **1–6** were characterized by HRMS, ^{1}H, ^{13}C, ^{19}F and ^{11}B spectroscopy (ESI†). Molecular ion peaks in HRMS spectra of bis-dipyrranes **7–10** and bis-BODIPYs **1–6** confirmed the formation of these compounds (ESI†). Also, single crystal X-ray structures were solved for bis-BODIPYs **1**, **2** and **4**. Typically in the ^{1}H NMR spectra of bis-dipyrranes **7–10** the four N–H protons appeared around 7.8–7.9 ppm as one singlet. The four α-pyrrole protons showed up between 6.65–6.83 ppm, whereas eight β-pyrrole protons gave two separate signals around 5.92–6.14 ppm. The two protons attached to sp^3 hybridized carbon (C–H protons) appeared around 5.45–5.29 ppm as one singlet (ESI†). The appearance of characteristic signals for the aromatic protons present in bridging units also confirmed the formation of bis-dipyrranes **7–10**. The formation of bis-BODIPYs **1–6** was

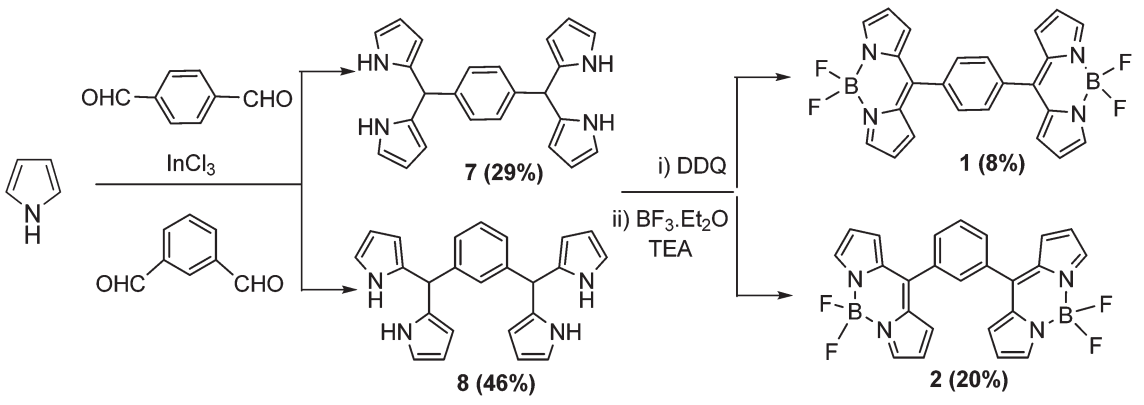

Scheme 1 Synthetic route for bis-BODIPYs **1** and **2**.

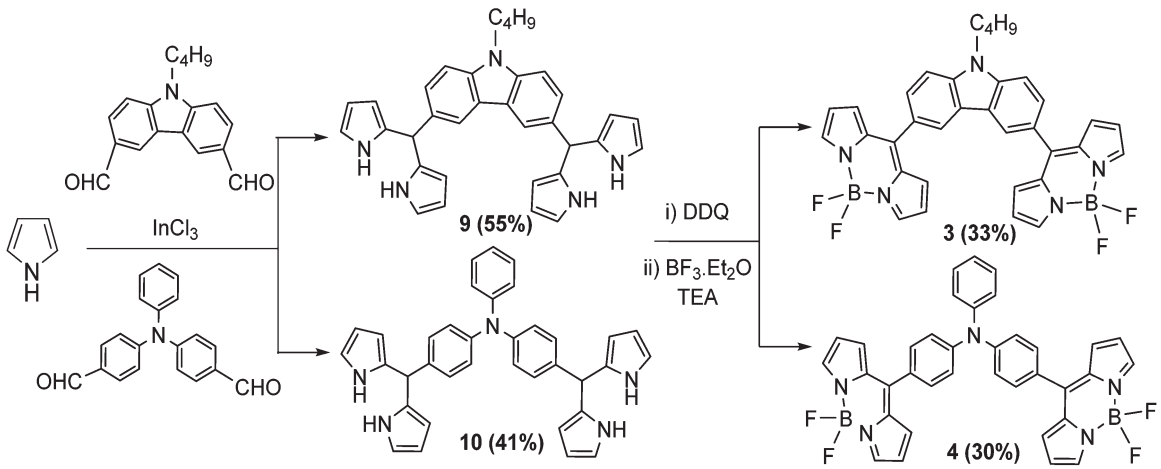

Scheme 2 Synthetic route for bis-BODIPYs **3** and **4**.

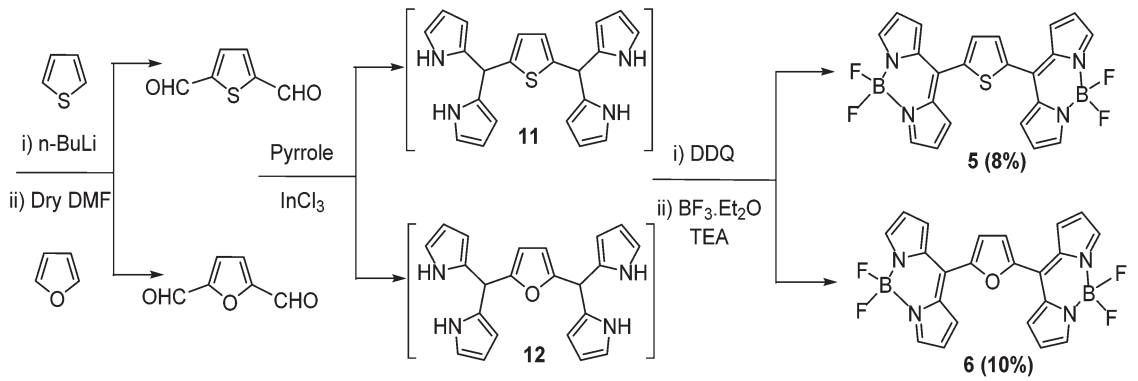

Scheme 3 Synthetic route for bis-BODIPYs **5** and **6**.

evident in their ^{1}H NMR spectra. The representative ^{1}H, ^{19}F and ^{11}B NMR spectra of bis-BODIPY **6** is presented in Fig. 1. Compared to the proton NMR spectra of their corresponding dipyrranes, two protons (C–H) attached to sp^{3} hybridized carbon and four N–H protons were missing in all the bis-BODIPYs **1–6**. In the proton NMR spectra of bis-BODIPY **6** (Fig. 1a) all the eight β-pyrrole protons appeared as two doublets at 6.64 and 7.68 ppm and the four α-pyrrole protons appeared as a singlet at 7.99 ppm. The two β-furan protons showed up as a singlet at 7.32 ppm. As compared to the corresponding bis-dipyrranes **7–10**, the four α-pyrrole proton signals were downfield shifted and appeared around 7.93–8.01 ppm in the bis-BODIPYs. In all bis-BODIPYs the eight β-pyrrole protons showed up as two separate signals between 6.61 and 7.02 ppm. In all the bis-BODIPYs the aromatic protons of bridging spacers showed up in the range of 7.29–7.59 ppm. The ^{19}F NMR spectra of all bis-BODIPYs **1–6** were recorded in $CDCl_3$ and fluorine resonance signals split into quartets due to the coupling with the adjacent boron atom (^{11}B, I = 3/2).[6] In ^{19}F NMR analysis of all bis-BODIPYs **1–6**, the ^{19}F quartets

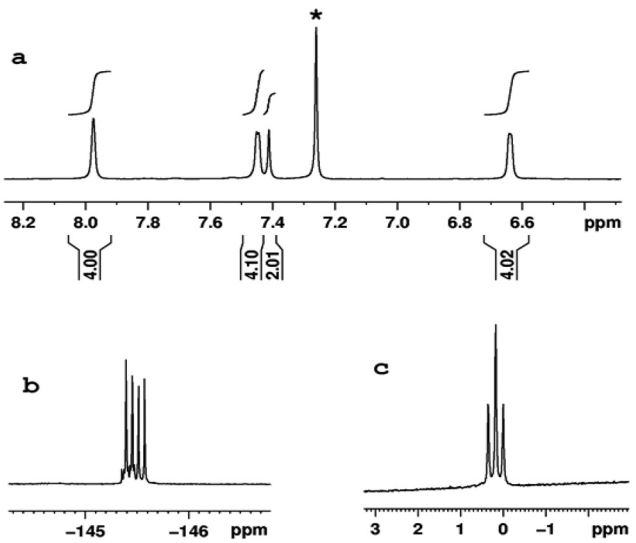

Fig. 1 The NMR spectra: (a) ^{1}H, (b) ^{19}F and (c) ^{11}B of bis-BODIPY **6** in $CDCl_3$.

appeared around −145 ppm and only one ^{19}F signal was observed due to the symmetrical nature of the molecules (Fig. 1b). ^{11}B NMR spectra of bis-BODIPYs **1–6** exhibited a triplet for ^{11}B between 0.18 and 0.36 ppm (Fig. 1c).

Single crystal X-ray diffraction studies

The X-ray structures of bis-BODIPYs **1**, **2** and **4** were determined. ORTEP views of bis-BODIPY **1**, bis-BODIPY **2** and bis-BODIPY **4** are given in Fig. 2. The single crystals of three bis-BODIPYs were obtained by slow evaporation of the chloroform/*n*-heptane solution over a period of two weeks. The crystal structure and data refinement parameters for **1**, **2** and **4** are displayed in ESI (Table S38†). Bis-BODIPY **1** (CCDC 1006185) gave red prism shaped crystals after solvent evaporation. Bis-BODIPY **1** was crystallised in a monoclinic crystal system with $P2_1/c$ space group. The values of N–B–N and F–B–F angles were 106.03° (12) and 109.12° (13) respectively. Here two boron dipyrrin units were aligned in the same plane and the bridging phenylene ring was in a different plane. The dihedral angle between the boron dipyrrin units and the phenylene ring (C4–C5–C11–C12) was 54.00° (18). The dihedral angle was comparatively lower than the *meso*-phenyl BODIPY[27] (the reported value was 60.80°). Bis-BODIPY **2** (CCDC 1006186) gave orange rectangle shaped crystals on crystal growth. The crystals were monoclinic type with $I2/a$ (#15) space group.

All three units in bis-BODIPY **2** (two boron dipyrrin units and one phenylene unit) were aligned in different planes. The dihedral angle between C4–C5–C11–C10 was 52.01° (17) and that between C6–C5–C11–C12 was 54.11° (18). This suggested that the inward angle was lower than the outward angle and thus the two boron-dipyrrin units are approaching closer to each other. The values of N–B–N and F–B–F angles were 105.54° (12) and 109.42° (12) respectively. Bis-BODIPY **4** (CCDC 1028232) gave orange needle shaped crystals. The crystals were again monoclinic type with $C2/c$ space group. The values of N–B–N and F–B–F angles were 106.21° (15) and 109.53° (17) respectively. The dihedral angles between the boron dipyrrins units and the triphenylamine unit were 44.60° (3) for C4–C5–C10–C11 and 45.50° (3) for C6–C5–C10–C15. These values were much lower than those of bis-BODIPYs **1** and **2**. The N–B–N and F–B–F angles in all three bis-BODIPYs were very similar to the reported *meso*-aryl BODIPY monomer. All three bis-BODIPYs **1**, **2** and **4** exhibited supramolecular interactions in their packing structures and the distances and angles of the interactions in the packing mode are presented in Table 1. Bis-BODIPY **1** has formed a layered structure in a 3D framework through weak hydrogen bonding (C–H···F) and C–H···π interactions (Table 1). In crystal packing, one layer was connected to the other *via* mutual C(2)–H (2)···π (pyrrolic) and C(10)–H (10)···π (pyrrolic) interactions (Fig. 3). In the packing

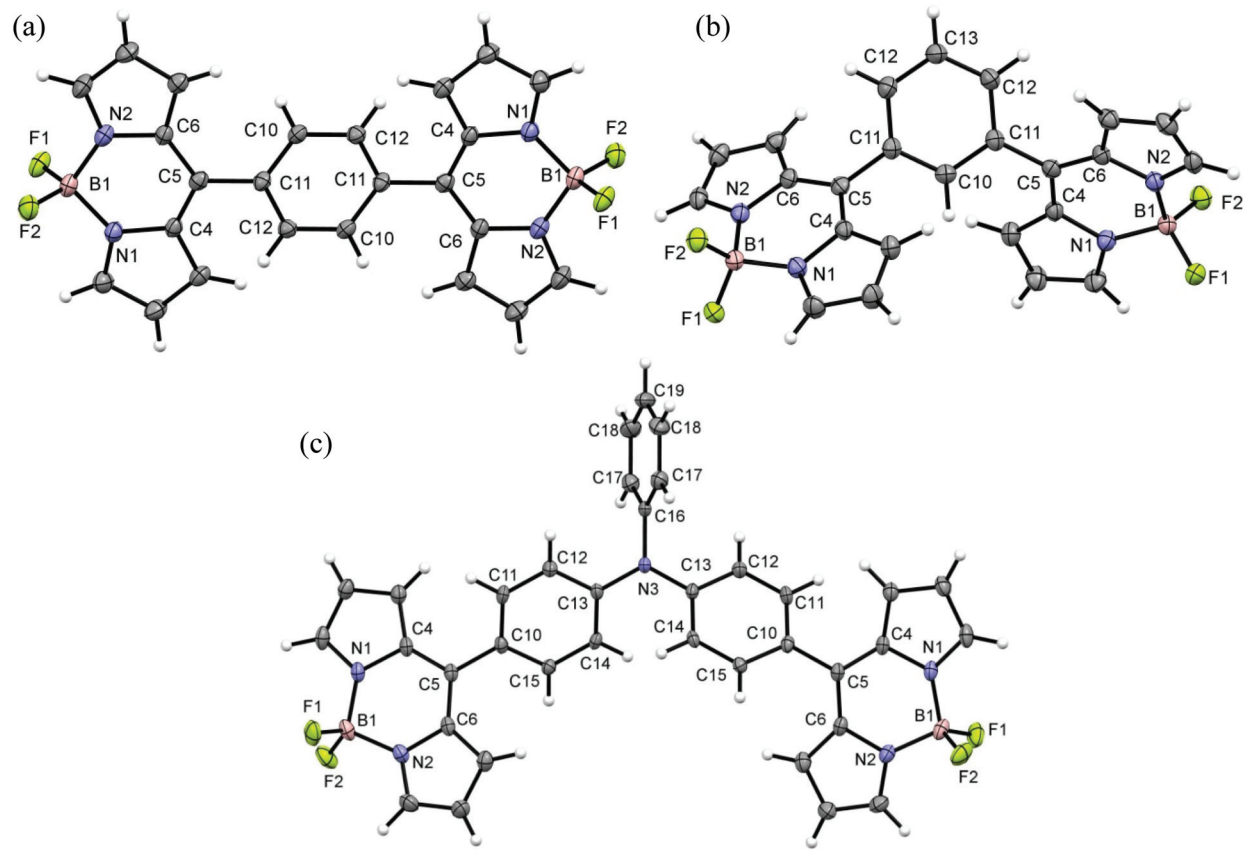

Fig. 2 ORTEP views of (a) bis-BODIPY **1**, (b) bis-BODIPY **2** and (c) bis-BODIPY **4**. Displacements are drawn at the 50% probability level.

Table 1 Details of intermolecular interactions in the crystal structures of bis-BODIPYs **1**, **2** and **4**

	No.	Interaction	Distance (Å)	Angle (°)
Bis-BODIPY **1**	1	C(1)–H(1)···π (C(12) phenyl))	2.69	141.73
	2	C(2)–H(2)···π (C(7) pyrrolic)	2.84	132.79
	3	C(3)–H(3)···B(1)	3.09	151.41
	4	C(3)–H(3)···F(1)	2.42	177.11
	5	C(7)–H(7)···F(1)	2.39	160.80
	6	C(10)–H(10)···π (C(3) pyrrolic)	2.71	173.93
	7	(C(1) pyrrolic) π···π (C(9) pyrrolic)	3.56(3)	—
	8	(C(2) pyrrolic) π···π (C(7) pyrrolic)	3.55(3)	—
Bis-BODIPY **2**	1	C(1)–H(1)···π(C(6) pyrrolic)	2.68	166.51
	2	C (1)–H(1)···N(2)	2.64	149.63
	3	C(3)–H(3)··· F(1)	2.30	164.40
	4	C(3)–H(3)···B(1)	3.06	138.83
	5	C(7)···F(1)	3.11(17)	—
	6	C(8)–H(8)···F(2)	2.58	117.53
	7	C(8)···F(2)	3.13(17)	—
	8	C(12)–H(12)···F(2)	2.64	143.28
	9	(C(1) pyrrolic) π···π (C(8) pyrrolic)	3.54(3)	—
	10	(C(1) pyrrolic) π···π (C(8) pyrrolic)	3.59(3)	—
	11	(C(2) pyrrolic) π···π (C(13) phenyl)	3.48(18)	—
Bis-BODIPY **4**	1	(C(1)Pyrrolic) π···π (C(11) phenyl)	3.26(4)	—
	2	C(8)–H(8)···F(2)	2.59	134.23
	3	C(11)–H(11)···F(1)	2.30	169.24
	4	C(12)–H(12)···F(2)	2.55	131.48
	5	(C(14) phenyl) π···π (C(15) phenyl)	3.31(3)	—
	6	(C(15) phenyl) π···π (C(15) phenyl)	3.33(3)	—
	7	C(19)–H(19)···π (C(14) phenyl)	2.79	146.83

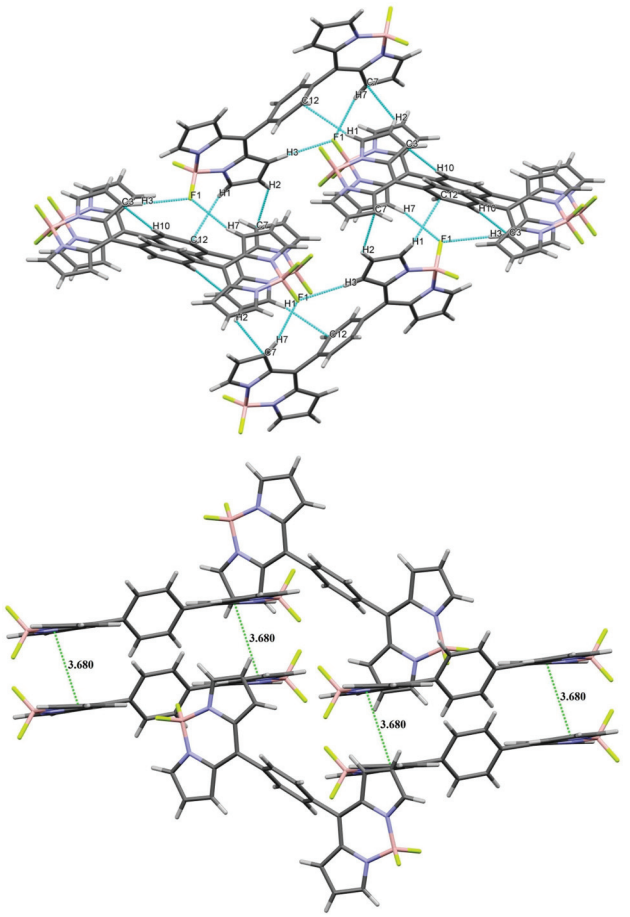

Fig. 3 Packing diagram (above) and π–π stacking diagram (below) of bis-BODIPY **1**.

diagram of bis-BODIPY **2**, molecules were connected through an antiparallel head to tail interaction *via* two mutual C(7)···F(1) interactions. Two boron dipyrrin units were connected to each other through C(3)–H(3)···F(1) and C(3)–H(3)···B(1) type weak intermolecular interactions to form a stacked 3D network (Fig. 4). One layer was also connected to the other through C(1)–H(1)···π (pyrrolic), C(1)–H(1)···N(2) and C(8)–H(8)···F(2) interactions (Fig. 4). The metric parameters for the interactions in bis-BODIPYs **1** and **2** were C–H···π (pyrrolic) distances 2.69 to 2.84 Å and C–H···π (pyrrolic) angles 132.79° and 173.93° respectively (Table 1). In the crystal packing mode of bis-BODIPY **4**, it formed a cluster of five molecules with the help of several intermolecular interactions (Fig. S37, ESI†). It included weak π···π interactions, hydrogen bonding and C–H···π interactions. These clusters were connected through C(11)–H(11)···F(1) to form the 3D structure of bis-BODIPY **4**.

Photophysical properties

UV-vis absorption and fluorescence studies. The UV/vis absorption, fluorescence spectra and fluorescence lifetimes of bis-BODIPYs **1–6** were examined in five different solvents. The absorption spectra of compounds **1–6** are presented in Fig. 5 and photophysical properties are summarized in Table 2. Bis-BODIPYs **1–4** showed a slight polarity dependence and exhibited a strong absorption band at around 500 nm with a shoulder at around 480 nm. The strong absorption at 500 nm is attributed to a strong S_0–S_1 electronic transition and the shoulder band corresponds to the S_0–S_1 vibrational transition. The broader and weaker band centred at 350 nm in bis-BODIPYs **1–2** and around 380 nm in bis-BODIPYs **3–4** was

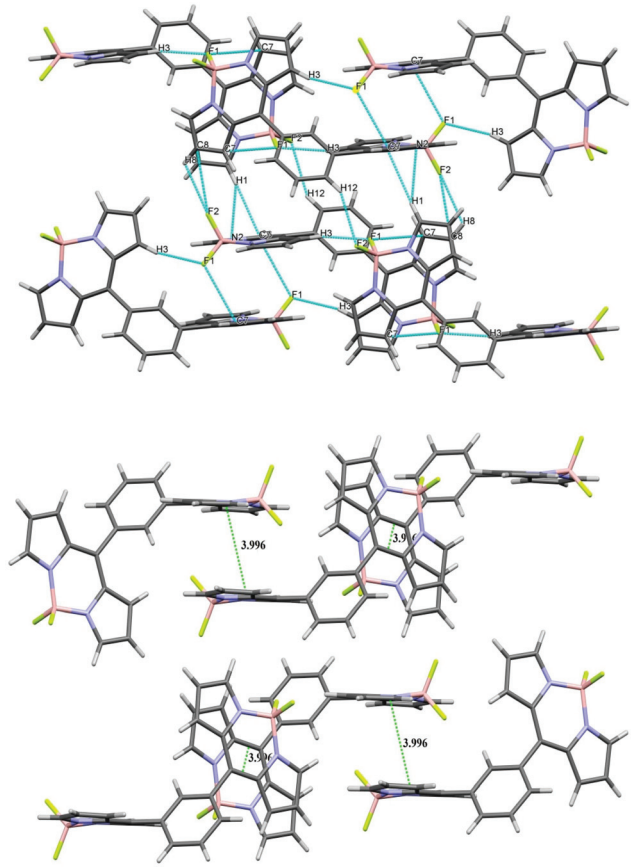

Fig. 4 Packing diagram (above) and π–π stacking diagram (below) of bis-BODIPY **2**.

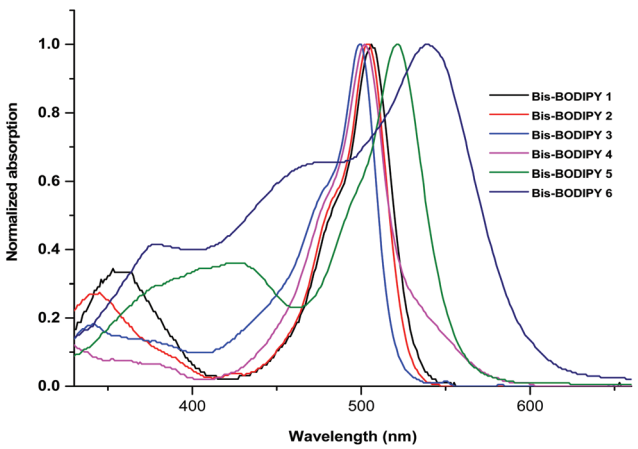

Fig. 5 Comparison of normalized absorption spectra of compounds **1–6** in chloroform.

assigned to the higher energy S_0–S_2 electronic transition. The wavelength of the major absorption band in bis-BODIPYs **1–2** in toluene was comparable with that of the *meso*-phenyl BODIPY monomer.[28] Also, the absorption maxima changed slightly (2–8 nm) upon changing the solvent polarity from toluene to acetonitrile (ESI†), reflecting the typical behavior of BODIPY chromophores.[11] The wavelength of the major absorption band of bis-BODIPYs **3** and **4** was similar to the corresponding *meso*-carbazole BODIPY (497 nm)[12] and *meso*-triphenylamine substituted BODIPY (500 nm).[29] Bis-BODIPYs **5** and **6** exhibited a 17 nm red shifted absorption band with a reduced extinction coefficient as compared to the corresponding *meso*-thienyl- and *meso*-furyl-BODIPY monomers,[30,31] shifted by 18 nm in the former. The $fwhm_{abs}$ (full width at half maxima of the major absorption band) of compounds **1–6** were calculated in different solvents (Table 2). Solvent polarity affected the broadening of the absorption band. Thus $fwhm_{abs}$ values of bis-BODIPYs **1–6** appeared as lower in the non-polar solvent (toluene) and higher in polar solvents (acetonitrile and tetrahydrofuran) for our compounds. This trend was in agreement with the *meso*-aryl BODIPYs. Compared to bis-BODIPYs **1–4**, bis-BODIPYs **5** and **6** showed more solvent polarity dependence. As the polarity of the solvent is increased, the absorption maxima were shifted to the blue region. Among all compounds, bis-BODIPY **6** showed significantly large $fwhm_{abs}$ values, which suggests that significant changes occurred in bond lengths/bond angles upon excitation.[32]

A comparison of emission spectra of **1–5** is shown in Fig. 6 and solvatochromism data are given in Table 2. The typical mirror-image relationship was observed for the lowest energy absorption band and emission spectra for bis-BODIPYs **1–5**. The emission maxima for compounds **1** and **2** were blue shifted by 41 and 34 nm respectively as compared to that of *meso*-phenyl BODIPY (in chloroform). The $fwhm_{em}$ (full width at half maxima of the emission band) and quantum yields of compounds **1–6** were calculated in different solvents (Table 2). Solvent polarity affected the broadening of the emission bands and typically $fwhm_{em}$ values were lower in the non-polar solvent (toluene) and higher in polar solvents for our compounds. The fluorescence quantum yields for bis-BODIPYs **1–2** were lower than those for *meso*-phenyl BODIPY (0.06 in toluene).[28] Usually the *meso*-aryl BODIPYs showed 10–15 nm Stokes shifts whereas these values were 26–33 nm for bis-BODIPYs **1** and **2**. In polar media red shifted emission maxima reflect larger dipoles of the CT excited states, which was in agreement with the report by N. Boens *et al.*[32] The fluorescence quantum yields for bis-BODIPY **3** and **4** were higher than those for the corresponding *meso*-carbazole- and *meso*-triphenylamine-BODIPY monomers.[12,29] The Stokes shift values were highest for compound **4** among all the bis-BODIPYs **1–6**. The emission maxima were red shifted for bis-BODIPYs **5** and **6** as compared to the corresponding *meso*-thienyl- and *meso*-furyl-BODIPY monomers. However, the quantum yields were lower for both bis-BODIPYs **5** and **6** as compared to their corresponding BODIPY monomers.[30,31]

Among all the bis-BODIPYs, compounds **3** and **4** showed higher quantum yields than **1–2** and **5–6**. Higher quantum yield indicates the possibility of restricted rotation of the two boron-dipyrrin units in bis-BODIPYs **3** and **4** due to bulky spacers; it was supported by the fact that much lower rate con-

Table 2 Photophysical data of compounds **1–6** in different solvents. The concentration used was 2.4×10^{-6} M

Compound	Solvent	λ_{abs} (nm)	fwhm$_{abs}$ (cm^{-1})	Log ε	λ_{emi} (cm^{-1})	fwhm$_{em}$ (cm^{-1})	$\Delta\nu_{st}$ (cm^{-1})	Φ_f	τ (ns)	k_r (10^9 s^{-1})	k_{nr} (10^9 s^{-1})
Bis-BODIPY **1**	Toluene	506	1510	4.63	539	1675	1210	0.014	0.08	0.18	10.75
	Dichloromethane	504	1485	4.46	531	1618	1009	0.012	0.07	0.17	14.11
	Chloroform	506	1516	4.59	534	1517	1036	0.015	0.08	0.19	12.31
	Tetrahydrofuran	503	1581	4.69	532	1731	1084	0.0085	0.06	0.14	16.53
	Acetonitrile	498	1610	4.75	526	1680	1069	0.0009	0.02	0.045	49.95
Bis-BODIPY **2**	Toluene	503	1497	4.82	529	1502	977	0.051	0.27	0.19	3.51
	Dichloromethane	502	1503	4.34	525	1335	873	0.042	0.26	0.16	3.68
	Chloroform	504	1534	4.89	527	1311	866	0.048	0.20	0.24	4.76
	Tetrahydrofuran	501	1638	4.52	525	1388	912	0.031	0.23	0.14	4.21
	Acetonitrile	496	1650	4.75	520	1428	931	0.009	0.04	0.23	24.78
Bis-BODIPY **3**	Toluene	—	—	—	—	—	—	—	—	—	—
	Dichloromethane	498	1630	4.66	581	3337	2869	0.173	2.90	0.06	0.29
	Chloroform	499	1724	4.74	517	2115	698	0.196	1.08	0.18	0.74
	Tetrahydrofuran	497	1637	4.91	569	3235	2546	0.18	0.07	0.07	0.30
	Acetonitrile	—	—	—	—	—	—	—	—	—	—
Bis-BODIPY **4**	Toluene	503	1659	4.88	585	1953	2787	0.41	3.43	0.12	0.17
	Dichloromethane	501	1724	4.69	680	2457	5254	0.018	2.18	0.008	0.38
	Chloroform	502	1666	4.80	633	2472	4123	0.135	4.12	0.033	0.21
	Tetrahydrofuran	500	1769	4.98	667	3981	5007	0.025	1.65	0.015	0.59
	Acetonitrile	495	1844	4.60	—	—	—	—	—	—	—
Bis-BODIPY **5**	Toluene	523	1796	4.28	531	3423	288	0.012	—	—	—
	Dichloromethane	520	1863	4.23	521	1977	37	0.009	0.03	0.3	33.03
	Chloroform	522	1772	4.30	529	2943	253	0.025	—	—	—
	Tetrahydrofuran	517	1895	4.42	524	2393	528	0.005	—	—	—
	Acetonitrile	513	1416	4.32	526	1993	482	0.0002	—	—	—
Bis-BODIPY **6**	Toluene	542	5313	4.18	633	—	2652	0.0018	—	—	—
	Dichloromethane	537	5235	4.15	627	—	2673	0.00087	0.06	0.0145	16.65
	Chloroform	539	5612	4.03	610	—	2159	0.0019	—	—	—
	Tetrahydrofuran	535	4983	4.33	576	—	1330	0.0016	—	—	—
	Acetonitrile	529	4831	4.05	577	—	1573	0.00038	—	—	—

$k_r = \Phi_f/\tau$ and $k_{nr} = (1 - \Phi_f)/\tau$.

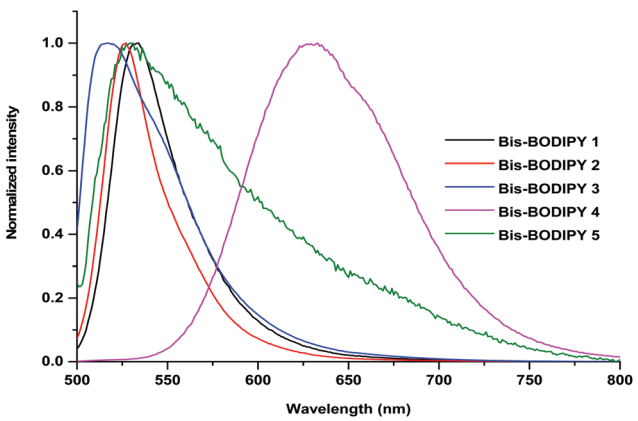

Fig. 6 Comparison of normalized emission spectra of compounds **1–5** in chloroform (λ_{ex} = 488 nm).

stant values (k_{nr}, see Table 2) were observed for non-radiative decay processes in these two compounds. The lower quantum yields for compounds **1**, **2**, **5** and **6** suggest that other non-radiative decay processes (such as internal conversion or inter-system crossing from S_1 to T_1) might be more feasible in these compounds.[27] Also, the quantum yields of bis-BODIPYs **5** and **6** being much lower than for other compounds could be associated with the electron donating ability of the heteroatom present in the bridging unit.[30] The quantum yields of bis-BODIPYs **1–6** were higher in the non-polar solvent (toluene) and lower in polar solvents (tetrahydrofuran); this is due to the large dipole moment difference between the CT excited state and the ground state which in turn facilitates internal conversion in polar media.[32] The time-correlated single photon counting technique was used to measure the singlet state lifetimes τ of bis-BODIPYs **1–6**. The fluorescence decay of compounds **1–4** was fitted to a single exponential decay (Fig. 7). However, in the case of bis-BODIPYs **5** and **6**, decay profiles fitted to three exponential decays (ESI†). The bridging phenylene unit is more rigid in bis-BODIPY **2** as compared to bis-BODIPY **1** (Table 2), thus the non-radiative decay processes are less prominent in **2**. It has been reported that the *meso*-mesityl-BODIPY showed higher quantum yields and singlet state lifetimes than *meso*-phenyl BODIPY, because the hin-

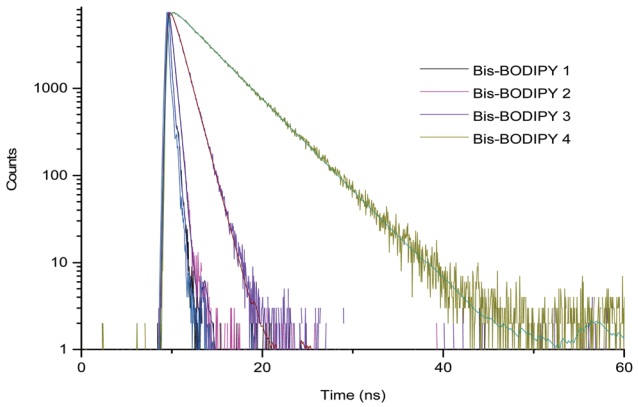

Fig. 7 Fluorescence decay profiles of compounds **1–4** in chloroform. The excitation wavelength was 515 nm, collected at their respective emission maxima.

dered rotation of the bulky mesityl group leads to a drastic decrease in the internal conversion process.[27] Therefore, the quantum yields and singlet state lifetimes of bis-BODIPY **2** are higher than those of bis-BODIPY **1**; this was again supported by the lower value of the non-radiative decay constant for **2** than **1** (Table 2). For bis-BODIPYs **1–4** singlet state lifetimes τ were lower than those for their corresponding BODIPY monomers. For example bis-BODIPY **3** has a lifetime of 1.9 ns in $CHCl_3$, whereas *meso*-carbazole BODIPY has 3.37 ns in the same solvent.[12] The decrease in radiative decay constant k_r and the increase in non-radiative decay constant k_{nr} were in line with the quantum yield data.

Computational details

The ground state geometry optimization of molecules **1–6** was performed with density functional theory (DFT) at the B3LYP/6-31G(d) level,[33–35] using the Gaussian 09 program package.[36] Frequency calculations were performed to guarantee that the optimized geometries are at energy minima on the potential energy surface. The vertical excitation energies were calculated employing the time dependent density functional theory (TD-DFT) approach at the same functional and basis sets.

Comparison of geometrical parameters

It is imperative to compare the vital structural parameters obtained as a result of geometry optimization of molecules **1**, **2** and **4** with the X-ray crystallography results (ESI†). To be more precise, the largest deviations in the bond lengths of molecules **1**, **2** and **4** are 0.017 Å, 0.025 Å and 0.021 Å respectively. The deviations from the X-ray geometry are reflected from the bond angles of the molecules (**1**, **2** and **4**) and are found to be 2.59°, 2.29° and 1.43° respectively. Moreover, the maximum deviations of the optimized dihedral angle in **1**, **2** and **4** are 6.14°, 12.54° and 8.87° respectively. The computed results compare well with the experimental data, thereby providing reliable support for the use of the selected level of theory for structural and spectroscopic studies of the rest of the molecules.

Absorption studies

To gain detailed insights into the roots of absorption bands the singlet–singlet transitions of BODIPY molecules were simulated using the TD-DFT/B3LYP level of theory at the valence double-ζ 6-31G(d) basis set. The gas phase determined electronic spectra exhibit a number of absorption peaks, and the peaks with maximum wavelength absorption (λ_{max}) were selected for the comparison. The effect of solvent polarities has not been taken into account as is obvious from the experimental results. The ineffectiveness of the solvent polarity on λ_{max} excludes any ground state intramolecular charge transfer (ICT) process of the molecules under consideration.[37] The lowest energy absorption maxima of molecules **1–6** are summarised in Table 3. The λ_{max} of **1**, **2**, **3** and **4** were observed at around 500 nm and for **5** and **6**, the red-shifted bands at 522 and 539 nm respectively indicate a lower HOMO–LUMO gap, which is supported by DFT studies. The delocalization of frontier molecular orbitals (FMOs) of compounds **1–6** indicated a significant electronic conjugation between the boron dipyrrin units and the spacers. Interestingly the HOMO–LUMO gap for **6** (2.513 eV) is less than that of **1** (2.877 eV), **2** (3.040 eV), **3** (3.050 eV), **4** (2.812 eV) and **5** (2.770 eV). Though DFT produced HOMO–LUMO gaps do not directly corroborate the experimentally observed (UV-Vis) energy gap values, almost the same trend of band gap increment (**3** > **2** > **1** > **4** > **5** > **6**) is reflected. For bis-BODIPY **3**, in spite of the highest HOMO energy level, the most destabilized LUMO resulted in its highest HOMO–LUMO gap. On the other hand, for bis-BODIPY **6**, the destabilization of the LUMO is considerably lower because of approximately planar arrangement of the furan spacer increasing the level of effective conjugation, resulting in a HOMO–LUMO gap that is lower than the rest of molecules **1**, **2**, **3**, **4** and **5**.

The frontier molecular orbitals of molecules **1–6** are displayed in Fig. 8. The distribution of HOMO and LUMO reflects the strong donor–acceptor interactions. In bis-BODIPYs **1**, **2**, **3** and **5**, the HOMO was localized on the BODIPY moiety and the LUMO was shifted to the corresponding spacer groups. On the other hand in **4** and **6**, the HOMO was localized on the spacer moieties whereas the LUMO was budged to the BODIPY

Table 3 Absorption data of bis-BODIPYs **1–6**

	Experimental λ_{max} (nm)	Log ∈	Calculated λ_{max} (nm)	(F)
Bis-BODIPY **1**	506	4.59	472.02	0.0631
Bis-BODIPY **2**	504	4.89	466.98	0.0029
Bis-BODIPY **3**	499	4.74	445.05	0.2490
Bis-BODIPY **4**	502	4.80	520.17	0.0411
Bis-BODIPY **5**	522	4.30	493.65	0.0390
Bis-BODIPY **6**	539	4.03	541.08	0.0440

∈ is the molar extinction coefficient and F is the oscillator strength.

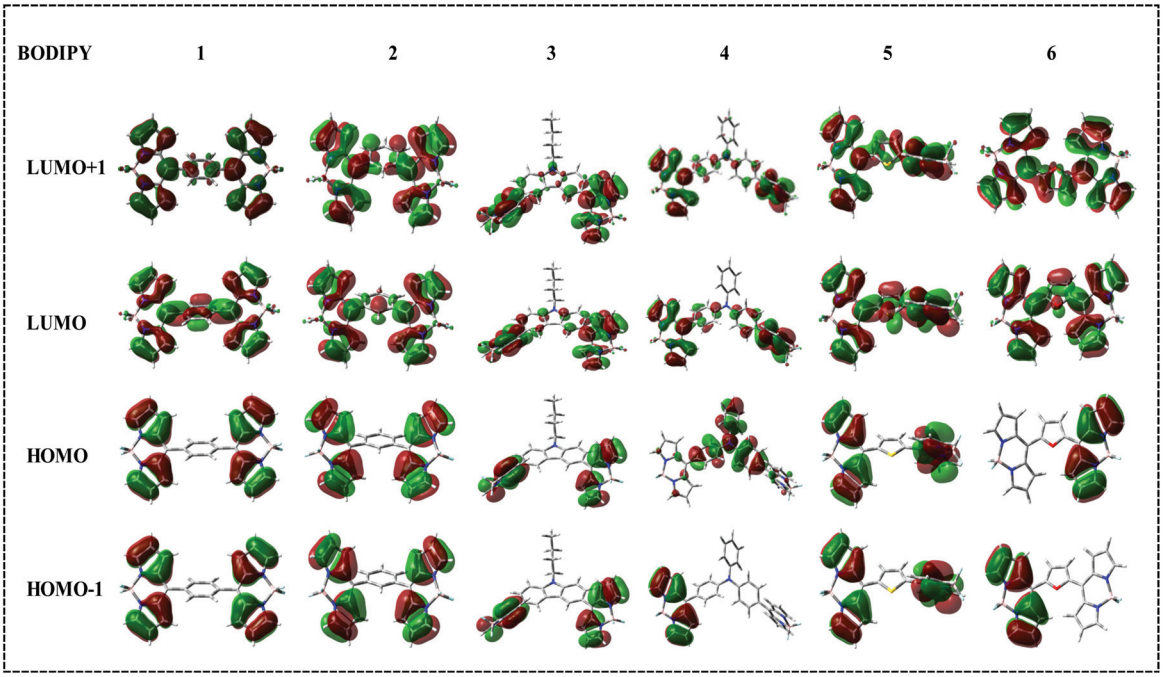

Fig. 8 Frontier molecular orbitals of bis-BODIPYs **1–6** at the B3LYP/6-31G(d) level for all the atoms.

moiety. The major absorption band in the electronic absorption spectra of molecules **1–6** is related to the BODIPY absorption which reflects that the origin of major absorption peaks is from HOMO energy levels. It can be seen that the TD-DFT calculations were in good agreement with the experimental results and unveil that the main transitions for **1**, **2**, **3**, **4**, **5** and **6** are from HOMO → LUMO, HOMO → LUMO+1, HOMO → LUMO+1, HOMO → LUMO, HOMO → LUMO and HOMO → LUMO+1 respectively.

Electrochemical studies

The cyclic voltammetry measurements of bis-BODIPYs **1–6** were carried out at a scan rate of 50 mV s^{-1} using tetrabutylammonium perchlorate (TBAP) as a supporting electrolyte. The redox potential data and a comparison of reduction waves are summarised in Table 4 and Fig. 9 respectively. All the bis-BODIPYs showed only reduction peaks. Bis-BODIPY **1** showed two reduction peaks. The first reduction peak was chemically reversible at −0.49 V and the other one was chemically irreversible around −1.75 V. Bis-BODIPY **2** showed three reduction waves, two reversible and one irreversible.

The reported *meso*-tolyl BODIPY monomer showed two reduction peaks at −0.788 and −1.81 V. As compared to the reduction potentials of *meso*-tolyl BODIPY,[31] the first reduction potential of both bis-BODIPYs **1** and **2** exhibited an anodic shift, *i.e.* they were much easier to reduce compared to the monomer *meso*-tolyl BODIPY. Bis-BODIPY **3** also showed two reduction waves. The first reduction potential of bis-BODIPY **3** was shifted towards the less negative side by 50 mV as compared to its corresponding monomer.[12] This reflects that compound **3** was much easier to reduce compared to the monomer. Bis-BODIPY **4** also showed two reduction waves with a reduction potential of −0.64 V and −1.36 V. Bis-BODIPYs **5** and **6** showed single reduction waves with a reduction potential of around −0.17 V. The reported first reduction potential for monomeric *meso*-furyl BODIPY was −0.66 V.[31] The electrochemical study of compounds **1–6** suggests that compared to their corresponding BODIPY monomers, the reduction potentials of **1–6** were low and they were very easy to reduce.

Table 4 Electrochemical redox data (V) of compounds **1–6** in dichloromethane containing 0.1 M TBAP as the supporting electrolyte recorded at 50 mV s^{-1} scan speed

	E_{red} (V *vs.* SCE)		
	I	II	III
Bis-BODIPY **1**	−0.49	−1.75	—
Bis-BODIPY **2**	−0.55	−0.67	−1.67
Bis-BODIPY **3**	−0.66	−1.72	—
Bis-BODIPY **4**	−0.64	−1.36	—
Bis-BODIPY **5**	−0.17	—	—
Bis-BODIPY **6**	−0.17	—	—

Conclusion

In conclusion, we have synthesized and characterized six borondipyrrins containing a bridging arene or heterocyclic ring. Their absorption, emission, electrochemical and time resolved

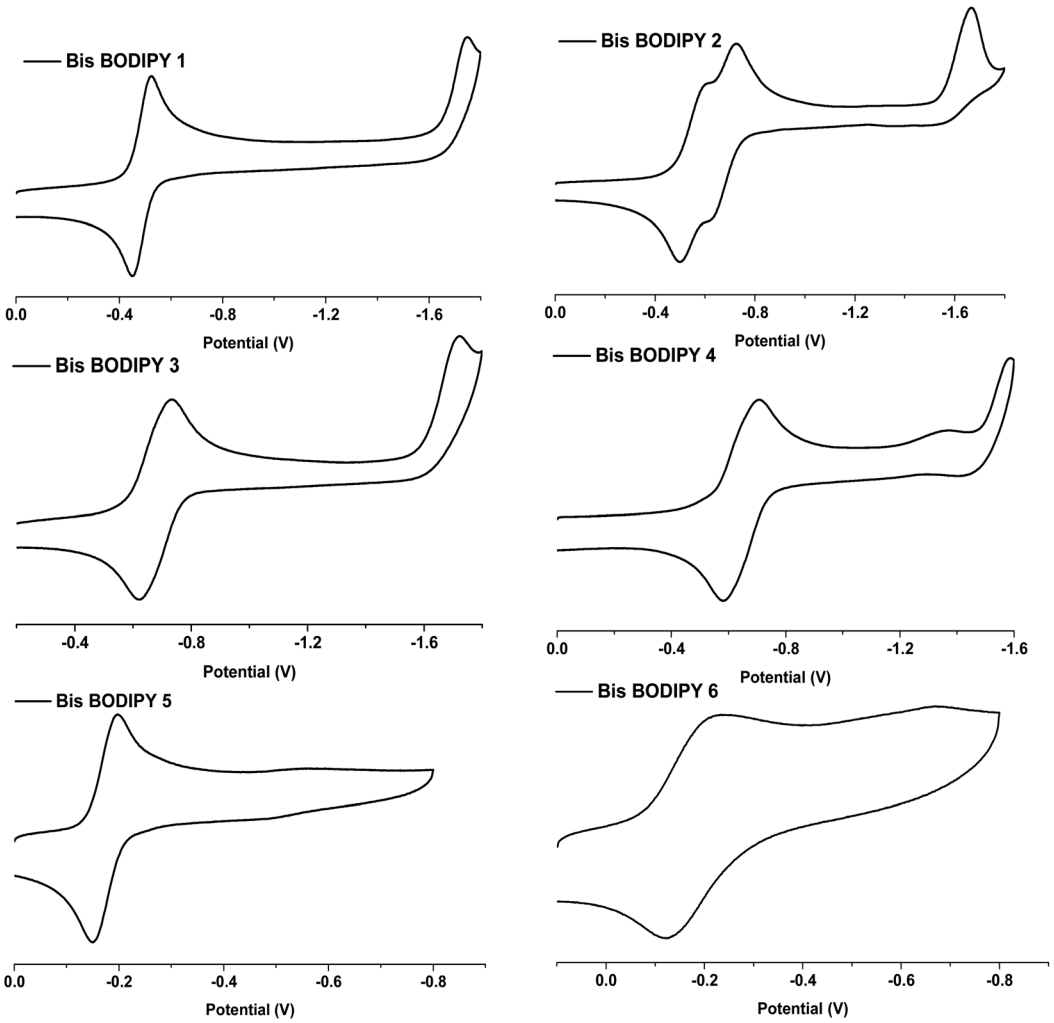

Fig. 9 Comparison of cyclic voltammograms of compounds **1–6** in dichloromethane, containing 0.1 M TBAP as the supporting electrolyte recorded at 50 mV s^{-1} scan speed (V *vs.* SCE).

florescence studies were carried out. Changing the spacer size from bulky carbazole to phenylene to smaller thiophene and furan rings affected the spectroscopic properties of bis-BODIPYs. The absorption and emission maxima were blue shifted for bis-BODIPYs having bulky aromatic spacers and red shifted for bis-BODIPYs having smaller thiophene/furan spacers. Also, the X-ray crystal structures of three bis-BODIPYs were solved. The reduced dihedral angle between the bridging ring and the dipyrrin core in all three crystal structures indicated better interactions between the two constituting boron dipyrrin units. Also, phenyl bridged bis-BODIPYs showed C–H···π (pyrrolic) and π···π interactions in 3D structures. DFT calculations showed the largest HOMO–LUMO gap for **3** and the lowest one for **6**. Also, gas phase absorption maxima calculated for **1–6** were closer to the experimental values. The observed anodic shifts in the reduction potentials of all six bis-BODIPYs suggested increased electronic interactions between two boron dipyrrin units within the molecule. Also, as compared to their corresponding monomer BODIPYs all six bis-BODIPYs were easier to reduce.

Experimental

General methods and reagents

Unless otherwise mentioned, all the reagents and solvents were purchased from Aldrich, Acros Organics or Merck and used without further purification. Pyrrole was distilled under vacuum prior to use. Silica gel (60–120 mesh size) used for column chromatography were procured from Merck. The solution NMR spectra of the compounds were recorded with a Bruker Avance III 500 MHz NMR spectrometer at IIT Gandhinagar. Absorption spectra were recorded with a Shimadzu UV-1700 and fluorescence emission studies were performed using a Horiba-Jobin Yvon Fluorolog-3 spectrometer at IIT Gandhinagar. The fluorescence quantum yields (Φ_f) were estimated from the emission and absorption spectra by a comparative method at the excitation wavelength of 488 nm using Rhodamine B (Φ_f = 0.49) in ethanol as the standard. The time-resolved fluorescence decay measurements were carried out at IIT Gandhinagar using a pico-second-diode-laser-based,

time-correlated, single-photon counting (TCSPC) fluorescence spectrometer from Edinburgh Instruments Ltd, LifespecII (Livingston, UK). Cyclic voltammetric (CV) studies were carried out with an electrochemical system utilizing the three electrode configuration consisting of a glassy carbon (working electrode), platinum wire (auxiliary electrode) and saturated calomel (reference electrode) electrodes. The experiments were done in dry dichloromethane using 0.1 M tetrabutylammonium perchlorate as the supporting electrolyte. All potentials were calibrated *vs.* a saturated calomel electrode by the addition of ferrocene as an internal standard, taking $E_{\frac{1}{2}}$ (Fc/Fc^+) = 0.51 V *vs.* SCE.

Synthesis of bis-dipyrrane 7. To a stirred solution of terephthalaldehyde (500 mg, 3.72 mmol) and pyrrole (38.79 mL, 559.14 mmol), acid catalyst ($InCl_3$, 82.49 mg, 0.37 mmol) was added at room temperature. The reaction mixture was allowed to stir for 2 h at room temperature under a N_2 atmosphere. After stirring for 2 h, excess pyrrole was removed by distillation under reduced pressure. The crude residue was dissolved in a small amount of dichloromethane and purified by column chromatography on silica gel (ethyl acetate/dichloromethane/hexane = 1 : 2 : 4) to give **7** as a pale yellow powder. Yield: 29% (400 mg). ^{1}H NMR (500 MHz, $CDCl_3$, δ ppm): 7.921 (bs, 4H), 7.170 (s, 4H), 6.695–6.692 (d, J = 1.5 Hz, 4H), 6.160–6.143 (m, 4H), 5.914 (s, 4H), 5.45 (s, 2H). HRMS [ESI]: calcd for $C_{24}H_{21}N_4$ $[(M - H)^+]$: m/z 365.1766, obsvd: m/z 365.1769.

Synthesis of bis-dipyrrane 8. Isophthalaldehyde (600 mg, 4.47 mmol) and pyrrole (150 eq., 46.5 mL, 670 mmol) were taken in a 100 mL round bottom flask and stirred for 5 minutes under nitrogen at room temperature. After stirring for 5 min $InCl_3$ (0.1 eq., 98.91 mg, 0.44 mmol) was added and the reaction mixture was allowed to stir for another 2 h. By vacuum distillation, excess pyrrole was removed. The crude mixture was subjected to silica gel column chromatography (ethyl acetate/dichloromethane/hexane = 1 : 2 : 4) to isolate the desired compound **8** as a sticky yellow solid in 46% yield (750 mg). ^{1}H NMR (500 MHz, $CDCl_3$, δ ppm): 7.862 (bs, 4H), 7.263–7.233 (t, J = 6 Hz 1H), 7.121 (s, 1H), 7.089–7.074 (dd, 2H), 6.654–6.651 (d, J = 1.5 Hz, 4H) 6.140–6.123 (m, 4H), 5.864 (s, 4H), 5.367 (s, 2H). HRMS [ESI]: calcd for $C_{24}H_{21}N_4$ $[(M - H)^+]$: m/z 365.1766, obsvd: m/z 365.1769.

Synthesis of bis-dipyrrane 9. *N*-Butylcarbazole-bis-aldehyde (500 mg, 1.78 mmol) was dissolved in pyrrole (150 eq., 18.63 mL, 268.51 mmol) under a nitrogen atmosphere. After 5 min $InCl_3$ (0.1 eq. 39.49 mg, 0.18 mmol) was added and the reaction mixture was allowed to stir for 2 h. Excess pyrrole was removed by vacuum distillation. The desired compound **9** was isolated *via* column chromatography (ethyl acetate/dichloromethane/hexane = 5 : 20 : 75) in 55% yield (550 mg). ^{1}H NMR (500 MHz, $CDCl_3$, δ ppm):7.94 (s, 4H), 7.32 (s, 4H), 6.68 (s, 4H), 6.16 (d, J = 3 Hz, 4H), 5.96 (s, 4H), 5.62 (s, 2H), 4.26 (t, J = 7 Hz, 2H), 1.82 (m, 2H), 1.41 (m, 2H), 0.93 (m, 3H). HRMS [ESI]: calcd for $C_{34}H_{32}N_5$ $[(M - H)^+]$: m/z 510.2658, obsvd: m/z 510.2657.

Synthesis of bis-dipyrrane 10. To a stirred solution of triphenylamine-bis-aldehyde (700 mg, 2.32 mmol) and pyrrole (24.12 mL, 347.68 mmol), $InCl_3$ (51 mg, 0.23 mmol) was added. The reaction mixture was protected from light and kept under stirring under nitrogen for 8 h at room temperature. After verifying the formation of the compound by TLC, excess pyrrole was vacuum distilled and the crude compound was subjected to silica gel column chromatography. The desired compound **10** was eluted with 60% dichloromethane/hexane. Yield: 41% (510 mg). ^{1}H NMR (500 MHz, $CDCl_3$, δ ppm): 7.93 (s, 4H), 7.07 (m, 7H), 7.00 (d, J = 8 Hz, 6H), 6.70 (s, 4H), 6.16 (d, J = 2.5 Hz, 4H), 5.93 (s, 4H), 5.41 (s, 2H). HRMS [ESI]: calcd for $C_{36}H_{32}N_5$ $[(M + H)^+]$: m/z 534.2658, obsvd: m/z 534.2664.

Synthesis of bis-BODIPY 1. Bis-dipyrrane **7** (200 mg, 0.54 mmol) was dissolved in dichloromethane (75 mL) and oxidized with DDQ (297 mg, 1.3 mmol, 2.4 eq.) at RT under air. The reaction mixture was allowed to stir at room temperature for 1 h. Triethylamine (6.1 mL, 80 eq.) followed by $BF_3{\cdot}Et_2O$ (6.80 mL, 100 eq.) was added to the reaction mixture successively without any time delay. The stirring was continued at room temperature for an additional 30 min, the reaction mixture was evaporated and the crude product was purified by silica gel column chromatography and eluted with a ethyl acetate/dichloromethane/petroleum ether (5 : 15 : 80) mixture to afford bis-BODIPY **1** as an orange powder in 8% yield (20 mg). ^{1}H NMR (500 MHz, $CDCl_3$, δ ppm): 8.008 (s, 4H), 7.761 (s, 4H), 7.002–6.994 (d, J = 3.5 Hz, 4H), 6.615–6.609 (d, J = 3 Hz). ^{13}C NMR (125.7 MHz, $CDCl_3$, δppm): 145.44, 144.96, 136.15, 134.77, 131.47, 130.49, 119.03. ^{19}F NMR (470.4 MHz, $CDCl_3$, δppm): −145.03 (q, 4F). ^{11}B NMR (160 MHz, $CDCl_3$, δ ppm): 0.29 (t, 2B). HRMS [ESI]: calcd for $C_{24}H_{16}B_2F_3N_4$ $[(M - F)^+]$: m/z 439.1513, obsvd: m/z 439.1520.

Synthesis of bis-BODIPY 2. Bis-dipyrrane **8** (200 mg, 0.54 mmol) was dissolved in dichloromethane (75 mL) and oxidized with DDQ (297 mg, 1.3 mmol, 2.4 eq.) at RT under air. The reaction mixture was allowed to stir at room temperature for 1 h. Triethylamine (6.1 mL, 80 eq.) and $BF_3{\cdot}Et_2O$ (6.8 mL, 100 eq.) were added to the reaction mixture without any time delay. The stirring was continued at room temperature for another 30 min; after this the reaction mixture was evaporated and the crude product was purified by silica gel column chromatography. The column was eluted with an ethyl acetate/dichloromethane/petroleum ether (5 : 15 : 80) mixture to afford bis-BODIPY **2** as an orange powder in 20% yield (50 mg). ^{1}H NMR (500 MHz, $CDCl_3$, δ ppm): 7.988 (s, 4H), 7.817–7.790 (t, J = 7.5 Hz, 3H), 7.745–7.715 (d, J = 7.5 Hz, 1H), 6.944–6.938 (d, J = 3 Hz, 4H), 6.593–6.589 (d, J = 2 Hz 4H). ^{13}C NMR (125.7 MHz, $CDCl_3$, δppm): 145.22, 145.01, 134.84, 134.27, 132.42, 131.87, 131.31, 128.76, 119.11. ^{19}F NMR (470.4 MHz, $CDCl_3$, δppm): −145.01 (q, 4F). ^{11}B NMR (160 MHz, $CDCl_3$, δ ppm): 0.26 (t, 2B). HRMS [ESI]: calcd for $C_{24}H_{16}B_2F_3N_4$ $[(M - F)^+]$: m/z 439.1513, obsvd: m/z 439.1520.

Synthesis of bis-BODIPY 3. Bis-Dipyrrane **9** (200 mg, 0.39 mmol) was dissolved in dichloromethane (54 mL) and oxidized with DDQ (213 mg, 0.94 mmol, 2.4 eq.) at RT under air. The reaction mixture was allowed to stir at room temperature for 1 h. Triethylamine (4.3 mL, 80 eq.) followed by $BF_3{\cdot}Et_2O$ (4.91 mL, 100 eq.) was added to the reaction mixture

without any time delay. The stirring was continued at room temperature for an additional 30 min, the reaction mixture was evaporated and the crude product was purified by silica gel column chromatography and eluted with a dichloromethane/petroleum ether (80 : 20) mixture to afford bis-BODIPY **3** as an orange powder in 33% yield (80 mg). ^{1}H NMR (500 MHz, $CDCl_3$, δ ppm): 8.385 (s, 2H), 7.954 (s, 4H), 7.804–7.787 (d, J = 8.5 Hz 2H), 7.637–7.620 (d, J = 8.5 Hz, 2H), 7.012–7.006 (d, J = 3 Hz, 4H), 6.579–6.575 (d, J = 2 Hz, 4H) 4.487–4.459 (t, J = 7 Hz, 2H), 2.016–1.987 (t, J = 7.5 Hz, 2H), 1.422–1.393 (t, J = 7 Hz, 2H), 1.067–1.038 (t, J = 7 Hz, 3H). ^{13}C NMR (125.7 MHz, $CDCl_3$, δ ppm): 143.40, 142.56, 135.19, 131.66, 129.53, 125.78, 123.63, 118.44, 109.29, 43.22, 31.21, 20.65, 13.89. ^{19}F NMR (470.4 MHz, $CDCl_3$, δ ppm): −145.10 (q, 4F). ^{11}B NMR (160 MHz, $CDCl_3$, δ ppm): 0.36 (t, 2B). HRMS [ESI]: calcd for $C_{34}H_{27}B_2F_4N_5$ [$(M - F)^+$]: m/z 584.2405, obsvd: m/z 584.2444.

Synthesis of bis-BODIPY 4. Bis-dipyrrane **10** (500 mg, 0.94 mmol) was dissolved in 75 mL of dichloromethane and oxidised with DDQ (511 mg, 2.27 mmol, 2.4 eq.) at room temperature under air. The reaction mixture was allowed to stir at RT for 1 h. After 1 h triethylamine (10.4 mL, 75 mmol, 80 eq.) followed by $BF_3{\cdot}Et_2O$ (8.13 mL, 94 mmol, 100 eq.) was added to the reaction mixture one by one without much time lag. The reaction mixture was allowed to stir at room temperature for 30 min; after this the solvent was evaporated and the crude product was purified by silica gel column chromatography. The desired compound bis-BODIPY **4** was eluted with an ethyl acetate/hexane (15 : 85) mixture in 30% yield (176 mg, reddish powder). ^{1}H NMR (500 MHz, $CDCl_3$, δ ppm): 7.937 (s, 4H), 7.557–7.540 (d, J = 8.5 Hz, 4H), 7.467–7.436 (t, J = 8.5 Hz, 2H), 7.306–7.275 (m, 7H), 7.063–7.057 (d, J = 3 Hz, 4H), 6.577–6.573 (d, J = 2 Hz, 4H). ^{13}C NMR (125.7 MHz, $CDCl_3$, δ ppm): 149.65, 146.89, 145.88, 143.51, 134.71, 132.30, 131.19, 130.19, 128.32, 126.94, 125.96, 122.55, 118.32. ^{19}F NMR (470.4 MHz, $CDCl_3$, δ ppm): −145.13 (q, 4F). ^{11}B NMR (160 MHz, $CDCl_3$, δ ppm): 0.29 (t, 2B). HRMS [ESI]: calcd for $C_{36}H_{25}B_2F_3N_5$ [$(M - F)^+$]: m/z 606.2248, obsvd: m/z 606.2269.

Synthesis of bis-BODIPY 5. Bis-dipyrrane **11** (400 mg, 0.28 mmol) and pyrrole (30 mL, 428 mmol) were stirred under nitrogen for 5 min. $InCl_3$ (6 mg, 0.03 mmol) was added and the reaction mixture was allowed to stir for a further 2 h. After 2 h excess pyrrole was vacuum distilled and the crude reaction mixture was dissolved in 50 mL of dichloromethane and oxidised with DDQ (292 mg) and allowed to stir for 1 h at RT. After 1 h, triethylamine (10.4 mL, 75 mmol, 80 eq.) and $BF_3{\cdot}Et_2O$ (8.13 mL, 94 mmol, 100 eq.) were added to the reaction mixture. The stirring was continued at room temperature for a further 30 min, and then reaction mixture was evaporated and the crude product was subjected to silica gel column chromatography. The desired compound was eluted in a dichloromethane/hexane (70 : 30) mixture in 8% yield (25 mg, dark orange powder). ^{1}H NMR (500 MHz, $CDCl_3$, δ ppm): 7.999 (s, 4H), 7.689 (s, 4H), 7.331–7.323 (d, J = 4 Hz, 4H), 6.652–6.645 (d, J = 3.5 Hz, 4H). ^{13}C NMR (125.7 MHz, $CDCl_3$, δ ppm): 145.16, 139.38, 137.26, 134.21, 132.86, 131.43, 119.22. ^{19}F NMR (470.4 MHz, $CDCl_3$, δ ppm): −145.13 (q, 4F). ^{11}B NMR (160 MHz, $CDCl_3$, δ ppm): 0.20 (t, 2B). HRMS [ESI]: calcd for $C_{22}H_{14}B_2F_3N_4S$ [$(M - F)^+$]: m/z 445.1077, obsvd: m/z 445.1107.

Synthesis of bis-BODIPY 6. The synthesis of bis-BODIPY **6** was performed by following a similar procedure to that used for bis-BODIPY **5**. Yield: 10% (25 mg) ^{1}H NMR (500 MHz, $CDCl_3$, δ ppm):7.976 (s, 4H), 7.452–7.445 (d, J = 3.5 Hz, 4H), 7.413 (s, 2H), 6.642–6.637 (d, J = 2.5 Hz, 4H). ^{13}C NMR (125.7 MHz, $CDCl_3$, δ ppm): 151.75, 144.70, 130.84, 121.23, 119.37. ^{19}F NMR (470.4 MHz, $CDCl_3$, δ ppm): −145.49 (q, 4F). ^{11}B NMR (160 MHz, $CDCl_3$, δ ppm): 0.18 (t, 2B). HRMS [ESI]: calcd for $C_{22}H_{14}B_2F_3N_4O$ [$(M - F)^+$]: m/z 429.1306, obsvd: m/z 429.1277.

Acknowledgements

IG gratefully acknowledges DST (New Delhi), CSIR (New Delhi) and IIT Gandhinagar for financial support. IG thanks the Chemistry Department, IIT Bombay for CV studies and Prof. H. Furuta, Kyushu University for X-ray measurements. PEK and SD thank IIT Gandhinagar for their fellowship. PCJ acknowledges CUG for providing basic computational facilities and UGC, New Delhi for start-up grants. MYL thanks UGC for fiscal assistance.

References

1 L. L. Shipman, T. M. Cotton, J. R. Norris and J. J. Katz, *Proc. Natl. Acad. Sci. U. S. A.*, 1976, **73**, 1791.
2 J. Deisenhofer, O. Epp, R. Miki, R. Huber and H. Michel, *J. Mol. Biol.*, 1984, **180**, 385.
3 J. Deisenhofer, O. Epp, R. Miki, R. Huber and H. Michel, *Nature*, 1985, **318**, 618.
4 M.-C. Yee, S. C. Fas, M. M. Stohlmeyer, T. J. Wandless and K. A. Cimprich, *J. Biol. Chem.*, 2005, **280**, 29053.
5 M. Fa, F. Bergstrom, P. Hagglof, M. Wilczynska, L. B. A. Johansson and T. Ny, *Structure*, 2000, **8**, 397.
6 J. Karolin, L. B. A. Johansson, L. Strandberg and T. Ny, *J. Am. Chem. Soc.*, 1994, **116**, 7801.
7 A. Kamkaew, S. H. Lim, H. B. Lee, L. V. Kiew, L. Y. Chung and K. Burgess, *Chem. Soc. Rev.*, 2013, **42**, 77.
8 Y. Wu, X. Peng, B. Guo, J. Fan, Z. Zhang, J. Wang, A. Cui and Y. Gao, *Org. Biomol. Chem.*, 2005, **3**, 1387.
9 Z. N. Sun, H. L. Wang, F. Q. Liu, Y. Chen, P. Kwong, H. Tam and D. Yang, *Org. Lett.*, 2009, **11**, 1887.
10 R. J. Middleton, S. J. Briddon, Y. Cordeaux, A. S. Yates, C. L. Cale, M. W. George, J. G. Baker, S. J. Hill and B. Kellam, *J. Med. Chem.*, 2007, **50**, 782.
11 K. Loudet and K. Burgess, *Chem. Rev.*, 2007, **107**, 4891.
12 P. E. Kesavan and I. Gupta, *Dalton Trans.*, 2104, **43**, 12405.
13 R. Ziessel and A. Harriman, *Chem. Commun.*, 2011, **47**, 611.
14 Y. Hayashi, S. Yamaguchi, W. Y. Cha, D. Kim and H. Shinokubo, *Org. Lett.*, 2011, **13**, 2992.

15 W. Pang, X. F. Zhang, J. Y. C. Zhou, A. Haoa and L. Jiao, *Chem. Commun.*, 2012, **48**, 5437.
16 Y. Cakmak, S. Kolemen, S. Duman, Y. Dede, Y. Dolen, B. Kilic, Z. Kostereli, L. T. Yildirim, A. L. Dogan, D. Guc and E. U. Akkaya, *Angew. Chem., Int. Ed.*, 2011, **50**, 11937.
17 L. Gai, B. Lu, B. Zou, G. Lai, Z. Shen and Z. Li, *RSC Adv.*, 2012, **2**, 8840.
18 A. Poirel, A. D. Nicola, P. Retailleau and R. Ziessel, *J. Org. Chem.*, 2012, **11**, 7512.
19 M. T. Whited, N. M. Patel, S. T. Roberts, K. Allen, P. I. Djurovich, S. E. Bradforth and M. E. Thompson, *Chem. Commun.*, 2012, **48**, 284.
20 S. Kusaka, R. Sakamoto, Y. Kitagawa, M. Okumura and H. Nishihara, *Chem. – Asian J.*, 2013, **8**, 723.
21 V. Yang, L. Li, B. Zhang, L. Zhanga and X. Liu, *RSC Adv.*, 2013, **3**, 16933.
22 H. Qi, J. J. Teesdale, R. C. Pupillo, J. Rosenthal and A. J. Bard, *J. Am. Chem. Soc.*, 2013, **135**, 13558.
23 A. V. Benniston, G. Copley, A. Harriman, D. Howgego, R. S. Harrington and W. Clegg, *J. Org. Chem.*, 2010, **75**, 2018.
24 N. Saki, T. Dinc and E. U. Akkaya, *Tetrahedron*, 2006, **62**, 2721.
25 H. Zhao, J. Liao, D. Yang, Y. Xie, Y. Xu, H. Wang and B. Wang, *Aust. J. Chem.*, 2013, **66**, 972.
26 R. W. Wagner and J. S. Lindsey, *Pure Appl. Chem.*, 1996, **68**, 1373.
27 H. L. Kee, C. Kirmaier, L. Yu, P. Thamyongkit, W. J. Younblood, M. E. Calder, L. Ramos, B. C. Noll, D. B. Bocian, R. Scheidt, R. R. Brige, J. S. Lindsey and D. Holten, *J. Phys. Chem. B*, 2005, **109**, 20433.
28 C. Yu, L. Jiao, H. Yin, J. Zhou, W. Pang, Y. Wu, Z. Wang, G. Yang and E. Hao, *Eur. J. Org. Chem.*, 2011, 5460.
29 E. Lager, J. Liu, A. Aguilar-Aguilar, B. Z. Tang and P. E. Cabrera, *J. Org. Chem.*, 2009, **74**, 2053.
30 K. Kim, C. Jo, S. Eswaramoorthi, J. Sung, D. H. Kim and D. G. Churchill, *Inorg. Chem.*, 2010, **49**, 4881.
31 T. K. Khan, S. K. Jana, M. R. Rao, M. S. Shaikh and M. Ravikanth, *Inorg. Chim. Acta*, 2012, **383**, 257.
32 W. Qin, M. Baruah, M. V. D. Auweraer, F. C. D. Schryver and N. Boens, *J. Phys. Chem. A*, 2005, **109**, 7371.
33 A. D. Becke, *J. Chem. Phys.*, 1993, **98**, 5648.
34 A. D. Becke, *Phys. Rev. A*, 1998, **38**, 3098.
35 A. D. Becke, *J. Chem. Phys.*, 1986, **84**, 4524.
36 M. J. Frisch, G. W. Trucos, H. B. Schlegel, G. E. Scuseria, M. A. Robb, J. R. Cheeseman, G. Scalmani, V. Barone, B. Mennucci and G. A. Petersson, *et al.*, *Gaussian 09 Revision A 02*, Gaussian Inc., Wallingford, CT, 2009.
37 A. S. P. Chinna, M. Sunoj and T. Pakkirisamy, *Inorg. Chem.*, 2014, **53**, 4813.